Temperature Oscillations Drive Cycles in the Activity of MMP-2,9 Secreted by a Human Trabecular Meshwork Cell Line

Stanley Ka-lok Li,[1,2] Juni Banerjee,[1] Christopher Jang,[3] Amita Sehgal,[4] Richard A. Stone,[5] and Mortimer M. Civan[1,6]

[1]Department of Physiology, University of Pennsylvania Perelman School of Medicine, Philadelphia, Pennsylvania, United States
[2]School of Optometry, The Hong Kong Polytechnic University, Hung Hom, Hong Kong
[3]Department of Biology, University of Pennsylvania, Philadelphia, Pennsylvania, United States
[4]Department of Neuroscience, University of Pennsylvania Perelman School of Medicine, Philadelphia, Pennsylvania, United States
[5]Department of Ophthalmology, University of Pennsylvania Perelman School of Medicine, Philadelphia, Pennsylvania, United States
[6]Department of Medicine, University of Pennsylvania Perelman School of Medicine, Philadelphia, Pennsylvania, United States

Correspondence: Mortimer M. Civan, Department of Physiology, University of Pennsylvania Perelman School of Medicine, A303 Richards Building, 3700 Hamilton Walk, Philadelphia, PA 19104-6085, USA; civan@mail.med.upenn.edu.

SKL and JB contributed equally to the work presented here and should therefore be regarded as equivalent authors.

Submitted: October 8, 2014
Accepted: January 26, 2015

Citation: Li SK, Banerjee J, Jang C, Sehgal A, Stone RA, Civan MM. Temperature oscillations drive cycles in the activity of MMP-2,9 secreted by a human trabecular meshwork cell line. *Invest Ophthalmol Vis Sci*. 2015;56:1396–1405. DOI:10.1167/iovs.14-15834

Purpose. Aqueous humor inflow falls 50% during sleeping hours without proportional fall in IOP, partly reflecting reduced outflow facility. The mechanisms underlying outflow facility cycling are unknown. One outflow facility regulator is matrix metalloproteinase (MMP) release from trabecular meshwork (TM) cells. Because anterior segment temperature must oscillate due to core temperature cycling and eyelid closure during sleep, we tested whether physiologically relevant temperature oscillations drive cycles in the activity of secreted MMP.

Methods. Temperature of transformed normal human TM cells (hTM5 line) was fixed or alternated 12 hours/12 hours between 33°C and 37°C. Activity of secreted MMP-2 and MMP-9 was measured by zymography, and gene expression by RT-PCR and quantitative PCR.

Results. Raising temperature to 37°C increased, and lowering to 33°C reduced, activity of secreted MMP. Switching between 37°C and 33°C altered MMP-9 by 40% ± 3% and MMP-2 by 22% ± 2%. Peripheral circadian clocks did not mediate temperature-driven cycling of MMP secretion because MMP-release oscillations did not persist at constant temperature after 3 to 6 days of alternating temperatures, and temperature cycles did not entrain clock-gene expression in these cells. Furthermore, inhibiting heat shock transcription factor 1, which links temperature and peripheral clock-gene oscillations, inhibited MMP-9 but not MMP-2 temperature-driven MMP cycling. Inhibition of heat-sensitive TRPV1 channels altered total MMP secretion but not temperature-induced modulations. Inhibiting cold-sensitive TRPM-8 channels had no effect.

Conclusions. Physiologically relevant temperature oscillations drive fluctuations of secreted MMP-2 and MMP-9 activity in hTM5 cells independent of peripheral clock genes and temperature-sensitive TRP channels.

Keywords: matrix metalloproteinases, trabecular outflow, circadian rhythm

The IOP is determined by the inflow rate of aqueous humor, the relative outflow through the higher-resistance trabecular pathway and lower-resistance uveoscleral pathway, and the episcleral venous pressure. Aqueous humor inflow falls by some 50% during nocturnal hours,[1] but is unaccompanied by a proportional reduction in IOP.[2–4] The relative constancy of IOP arises from an associated fall in outflow facility (equivalent to an increase in outflow resistance) and shunting of outflow from the uveoscleral to the trabecular outflow pathway during nocturnal hours.[4–6] Episcleral venous pressure is relatively constant if measured with the subject in the same position.[7] Despite sustained investigation, the triggers for the reduction in inflow[1] and the compensating falls in outflow facility and uveoscleral outflow are unknown.[4–6]

One potential link between the reductions in inflow and outflow facility might be a direct effect of reduced inflow to lower outflow facility by transiently reducing IOP. However, at least eight studies of human eyes ex vivo, thereby minimizing the roles of confounding variables, document that decreasing IOP does not consistently trigger a fall in outflow facility and increasing IOP does not consistently increase outflow facility.[8–15] Thus, reduced inflow is not expected to reduce outflow facility directly.

The basis for the nocturnal fall in inflow also is unclear. Many candidate mechanisms have been studied, including oscillations in melatonin level[1] and in sympathetic neural activity.[16] The inflow oscillations are circadian in humans and in laboratory animals.[1] Given the diurnal tracking of inflow rate and outflow facility, the nocturnal reduction in outflow facility might also reflect a circadian rhythm.

Circadian rhythms are approximately 24-hour endogenous rhythms in cellular, organ, and whole-body function orchestrated by transcription-translation feedback loops that constitute molecular clocks. In mammals, such clocks can be found

across the body, but the master or central clock is located in the hypothalamic suprachiasmatic nucleus (SCN). The SCN is reset by light and synchronizes other clocks to the day:night cycle. The primary loop of the molecular clocks consists of the transcription factors CLOCK and BMAL1 that interact with enhancer elements targeting transcription of the genes *Period1* (*Per1*), *Period 2* (*Per2*), *Cryptochrome1* (*Cry1*), and *Cryptochrome2* (*Cry2*).[17–19] In turn, the translated PER and CRY proteins inhibit CLOCK-BMAL1–triggered transcription, generating the circadian feedback loop.

A major signaling pathway by which the central clock of the hypothalamic SCN synchronizes the body's circadian rhythm is through cycling the core temperature by 2 to 4°C.[20,21] Ocular temperature also will cycle because of nocturnal eyelid closure.[22] The temperature oscillations can modulate cell function by acting directly on transient receptor potential (TRP) temperature-sensitive channels,[23] among other cell targets (see Discussion). In addition, the temperature cycling can synchronize the rhythms of the body's cells through peripheral clocks expressed in most cells and tissues.[20,21,24] Changes in temperature and peripheral circadian rhythm are likely linked through heat shock transcription factor 1 (HSF1), which also functions as a circadian transcription factor[20,21,25] (see Discussion).

In this work, we addressed the potential role of oscillating body temperature in driving a rhythm of aqueous humor outflow facility. We focused on outflow, because abnormally low values of outflow facility are usually associated with glaucoma, a major cause of irreversible blindness worldwide.[26] Although the site and mode of outflow facility regulation remain under active investigation, the extracellular matrix of the trabecular meshwork (TM) and juxtacanalicular tissue is thought to be a major contributor to this resistance. Increased matrix metalloproteinase (MMP) activity increases outflow facility,[27,28] and inhibiting endogenous trabecular MMP activity lowers outflow facility.[27] Separately and together, MMP-2 and MMP-9 increase outflow facility.[27] Here, we monitored secreted activity of MMP-2 and MMP-9 as indices of outflow facility regulation.

The primary question addressed is whether physiologically relevant temperature oscillations alter activity of MMP-2 and MMP-9 secreted by cultured human TM (hTM5) cells. As considered in the Discussion, it was unknown whether temperature cycling would drive activity of secreted MMP, and if so, in which direction. The results suggest that diurnal temperature cycling may be an important modulator of activity of MMP secreted by TM cells.

Materials and Methods

Cellular Model

As previously described,[29,30] the transformed TM cell line hTM5, derived from a healthy human donor (Alcon Research, Inc., Fort Worth, TX, USA), was maintained in Dulbecco's modified Eagle's medium (DMEM) high-glucose media supplemented with 10% fetal bovine serum (FBS) and 2 mM L-glutamine at 37°C in a humidified atmosphere of 5% CO_2 and 95% air. Cells from passages 30 to 38 were studied at 37°C and 33°C.

Solutions and Pharmacological Reagents

Unless otherwise stated, chemicals and media for cell culture were obtained from GIBCO (Grand Island, NY, USA). The DMEM with phenol red was purchased from Cellgro (Manassas, VA, USA). Dimethyl sulfoxide (DMSO) (Sigma-Aldrich Corp., St. Louis, MO, USA) was used to solubilize hydrophobic drugs, exposing controls to the same concentration of vehicle (<0.5%). Drugs and their sources were as follows: KNK437, an inhibitor of peripheral clock activation by preventing induction of heat shock transcription factor 1 (HSF1)[20,21] (Calbiochem, San Diego, CA, USA); BCTC, an inhibitor of TRPV1[31,32] and (in higher concentration) TRPM8[33] (Enzo Life Sciences, Inc., Farmingdale, NY, USA); and HC 067047, an inhibitor of TRPV4 and (in higher concentration) TRPM8 ion channels[34] (Santa Cruz Biotechnology, Inc., Dallas, TX, USA). The chemical names of KNK437, BCTC, and HC 067047 are N-formyl-3,4-methylenedioxy-benzylidine-gamma-butyrolactam, N-(4-tertiarybutylphenyl)-4-(3-cholorphyridin-2-yl)tetrahydropyrazine-1(2H)-carboxamide, and 2-methyl-1-[3-(4-morpholinyl)propyl]-5-phenyl-N-[3-(trifluoromethyl)phenyl]-1H-pyrrole-3-carboxamide, respectively.

Gelatin Zymography for MMPs

Using the previously reported method,[35–38] the activity of MMP-2 and MMP-9 secreted into the external media was measured by gelatin zymography. In our past[38] and present experience, the predominant form of the MMP-2 and MMP-9 secreted from human TM cells is in the proactive form and is therefore enzymatically inactive. However, zymograms measure enzyme activity of each secreted form of the MMPs because of enzyme activation during zymography. The secreted active forms of both MMPs on the gels were inconsistently visualized, and if present constituted only a small fraction of the total, and activity of the proform only was assessed in data reduction. Briefly, hTM5 cells were plated onto 48-well plates at a density of 62,500 or 120,000 per well. Unless otherwise stated, after incubation with 10% FBS for 12 hours, the FBS concentration was reduced to 1% throughout the control and experimental periods to suppress the rate of cell division. Further lowering the FBS concentration impaired TM-cell viability and was therefore not performed. After 24 hours at 1% FBS, cells were confluent. At that point, the media were replaced with 140 or 200 μL fresh DMEM, with or without drugs, for the periods specified. Every 12 hours, the conditioned media were completely collected and the wells replenished with fresh media. The collected media were cleared by centrifugation (14,000*g*) for 20 minutes. The supernatants were then mixed with the Zymogram Sample Buffer (Bio-Rad, Hercules, CA, USA), and 15 or 20 μL per sample was loaded onto each lane of the 10% polyacrylamide gels for SDS-PAGE separation. After electrophoresis, gels were washed sequentially with the Zymogram Renaturing Buffer (2.5% Triton X-100 aqueous solution) for 4 hours, Zymography Developing Buffer (25 mM Tris-HCl, 2.5 mM $CaCl_2$, 210 mM NaCl, and 25 μM $ZnSO_4$) for 18 to 24 hours (at 37°C), and Coomassie Brilliant Blue R-250 Staining Solution (Bio-Rad) overnight. Gels were destained in aqueous solution containing 10% ethanol and 10% acetic acid until clear bands were visible against the blue background. The gels were subsequently scanned (Scanjet 3570c; Hewlett-Packard, Palo Alto, CA, USA), and band density was analyzed by ImageJ software, version 1.45 (http://imagej.nih.gov/ij/; provided in the public domain by the National Institutes of Health, Bethesda, MD, USA).

Reverse-Transcription PCR for TRPV1-4 and Glyceraldehyde 3-Phosphate Dehydrogenase (GAPDH)

The RNA from hTM5 cells was isolated using an RNeasy kit (Qiagen, Valencia, CA, USA) and treated with RNase-free DNase I to avoid possible genomic DNA contamination, followed by reverse-transcription into cDNA by use of Taqman Reverse-

Transcription Reagents (Applied Biosystems [ABI], Foster City, CA, USA), according to the manufacturer's instructions. Polymerase chain reaction was performed with the AccuPrime Taq DNA polymerase High Fidelity Kit (Invitrogen, Carlsbad, CA, USA) according to the manufacturer's instructions. Polymerase chain reaction amplification was done using primers 5′-GCCTGGAGCTGTTCAAGTTC-3′ and 5′-TCTCCTGTGCGATCTTGTTG-3′ for TRPV1 (177 bp), 5′-CAAACCGATTTGACCGAGAT-3′ and 5′-GTTCAGCACAGCCTTC ATCA-3′ for TRPV2 (167 bp), 5′-ACGAGGCAACAACATCCTTC-3′ and 5′-CCGCTTCTCCTTGATCTCAC-3′ for TRPV3 (226 bp), 5′-GACGGGGACCTATAGCATCA-3′ and 5′-AACAGGTCCAGGA GGAAGGT-3′ for TRPV4 (228 bp), and 5′-CCATGGAGAAGG CTGGGG-3′ and 5′-CAAAGTTGTCATGGATGACC-3′ for GAPDH (194 bp).[39]

Polymerase chain reaction products were separated on 1% agarose gels containing 0.05% ethidium bromide. Bands were visualized under UV light, sized, and photographed. No product was detectable on omitting reverse-transcriptase (RTase[–]), confirming that the cDNA derived from total RNA was free of genomic DNA contamination.

Real-Time Quantitative PCR (qPCR)

As for RT-PCR (above), RNA was isolated using an RNeasy kit (Qiagen) following the manufacturer's protocol. The RNA was reverse-transcribed using a Superscript II First-Strand Synthesis kit (Invitrogen). A custom TaqMan quantitative real-time PCR (qRT-PCR) assay for two clock genes was performed using primers 5′-CCAGTGGACATGAGACCAAC-3′ and 5′-TTGCCATC ATCAGGCTAAAG-3′ for *Per2*; and 5′-AGGACTTGGTCCAG CTGTCT-3′ and 5′-GTTCATTCGGGGTCTCTCAT-3′ for *Cry2*, with 10 ng cDNA in a reaction volume of 25 μL. The probes were purchased, prevalidated from Integrated DNA Technologies, Inc. (Coralville, IA, USA). As an endogenous control, β-actin was used with primers 5′-CCAGTGGTACGGCCAG-3′ and 5′-GCGAGAAGATGACCCAGAT-3′. Other reaction components were provided by Applied Biosystems Power SYBR Green Universal Mastermix. TaqMan qRT-PCR reactions were carried out in 96-well plates using a 7300 Real-Time PCR System (Applied Biosystems) and default thermocycler program. Analysis was conducted by the ΔΔCt method.

Statistics

Analyses of variance and Student's *t*-test were performed with SigmaStat (Aspire Software International, Ashburn, VA, USA). After verification that the data passed normality and equal variance tests, Figures 1 to 3 were analyzed by two-way repeated measures ANOVA followed by the Holm-Sidak All Pairwise Multiple Comparison Procedures. Unless otherwise stated, the results are presented as means ± SE, with n and N indicating the number of wells or measurements in an individual experiment and the number of independent experiments performed, respectively. A probability (P) of the null hypothesis of less than 0.05 was considered statistically significant.

Results

Effect of Temperature Cycling on Activity of Secreted MMP-9 and MMP-2

In the experiment of Figure 1, cells were incubated during an initial baseline period (days 1–3) at 37°C. During the first 12 hours of the baseline period, the FBS concentration was 10%, and was thereafter reduced to 1%. After day 3, the culture was split into two independent sets of six wells of cells, with each set exposed to a temperature cycle of 12 hours at 33°C and 12 hours at 37°C. The two sets of cultures were maintained in reverse phases; one set was exposed to 33°C during daytime hours (daytime 33° protocol) and the other to 37°C (daytime 37° protocol). The cells experienced identical dark and light exposures; the term "daytime" here refers to the laboratory ambient "daytime" as a reference for the timing of temperature changes and not to any known circadian phase of the cells. Following 3 days of temperature cycling (days 4–7), each culture was incubated at constant temperature, 33°C for one and 37°C for the other. The media enriched over the preceding

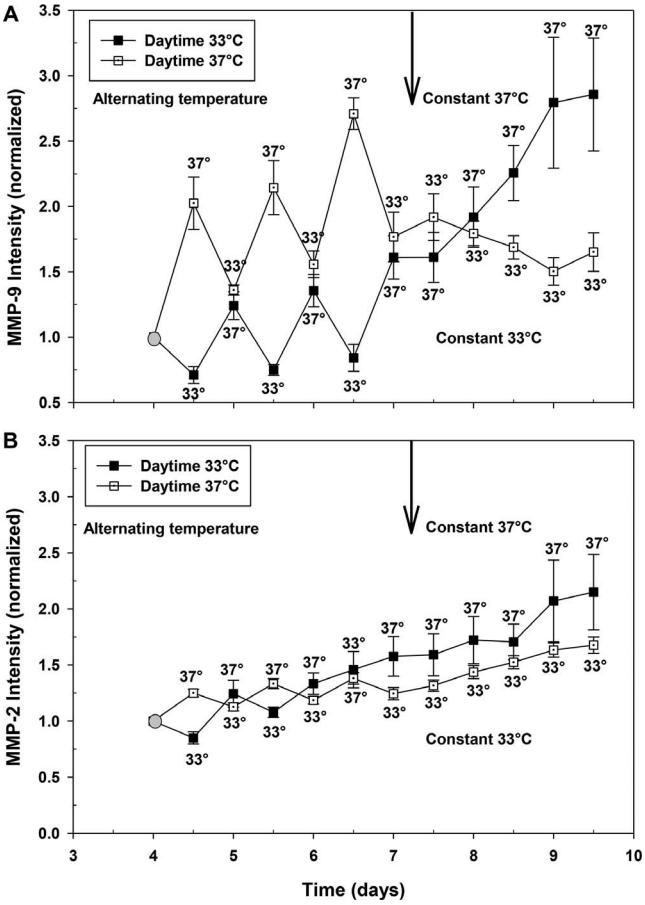

FIGURE 1. Enzyme activity of secreted MMP-9 (**A**) and MMP-2 (**B**) during and after 3 days of alternating temperature. Mean ± SE of 12-hour secretions from two plates of six wells of confluent hTM5 cells maintained in 1% FBS and cycled between 37 and 33°C, 12 hours out of phase with one another, for 3 days (days 4–7) before being clamped at 37 or 33°C (*vertical arrows*). Each *data point* is labeled with the incubation temperature during the preceding 12 hours. The first *data points* were obtained from enriched media collected at 9 AM of day 4 following 12 hours of nighttime incubation at either 33 or 37°C. The *open squares* (daytime 37°C) display relative secretory rates of the cells maintained at 37° during 9 AM to 9 PM; the *filled squares* (daytime 33°C) present the secretory rates of the cells whose temperature was 33°C during the same 12-hour period. Immediately after collection of the enriched media, the temperatures were switched, so that cells previously incubated at 33°C were maintained for the subsequent 12 hours at 37°C, and vice versa. Replicate measurements were taken from each well at each time point and averaged to generate the figure. Subsequent *data points* are connected for each set and normalized to the zymographic intensity of the first measurement of that set (symbolized by the *gray-filled circle* at day 4.0). The temperature-driven oscillations in secretion were diminished or absent after clamping the temperature at either 37°C or 33°C (see text).

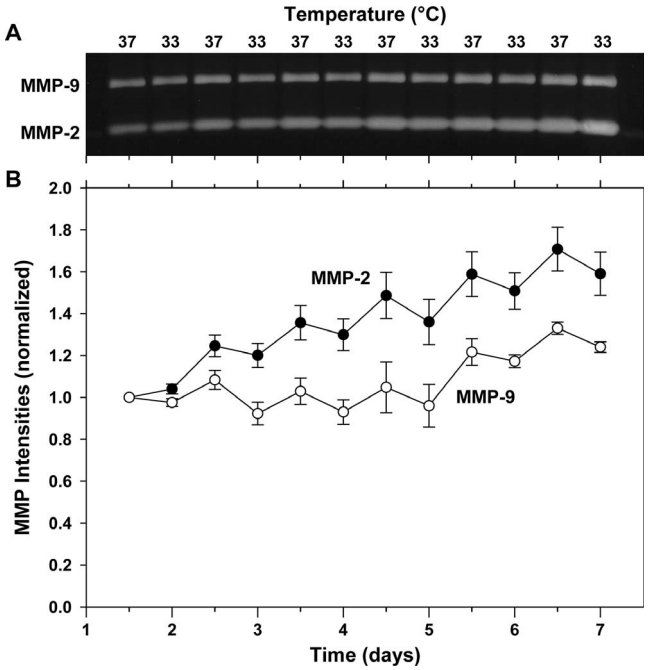

FIGURE 2. Enzyme activity of secreted MMP-9 and MMP-2 during 6 days of alternating temperature. As in Figures 1A and 1B, the mean ± SE of relative MMP intensities (**B**) have been calculated from replicate measurements of media from four wells, enriched over the preceding 12 hours at either 37°C or 33°C. The temperatures during those collections are indicated at the *top* of (**A**), which also presents a representative zymogram from one of the wells included in the averaged data of (**B**). The bands of (**A**) are centered over the time point at which the enriched media were collected, and display greater height and intensity at the higher temperature. Two-way repeated measures ANOVA of the scanned band intensities indicates that the relative intensities of both MMP-9 ($P = 0.001$) and MMP-2 ($P < 0.001$) were larger at 37°C than at 33°C.

12 hours were collected at the times indicated in Figure 1, following which the temperature was switched. The reverse temperature cycles of the two sets of wells provided verification that observed differences in activity of secreted MMP did not depend on length of incubation, order of alternating the temperature, light exposure, or other confounding variables.

As illustrated by Figure 1, some degree of upward drift was displayed by the normalized intensity in all experiments, perhaps reflecting incomplete suppression of cell division even at 1% FBS. Nevertheless, we detected oscillations in activity of secreted MMP-9 (Fig. 1A) and MMP-2 (Fig. 1B) that were synchronous with the temperature cycling. Activity of secreted MMP was consistently higher during 12-hour incubations at 37°C than at 33°C, irrespective of protocol. Analysis was conducted with two-way repeated measures ANOVA, with temperature and day as the two factors. The effect of temperature was significant for both MMP-9 (daytime 33°C, $P = 0.003$ and daytime 37°C, $P = 0.002$, Fig. 1A) and MMP-2 (daytime 37°C, $P < 0.001$, Fig. 1B). Temperature did not significantly affect the daytime 33°C measurements of MMP-2 secretion in Figure 1B ($P = 0.146$). In all experiments, the relative effect on MMP-9 was either greater than (Fig. 1) or equal to (Figs. 2–3) that on MMP-2. At the time of the vertical arrows in Figures 1A and 1B, the temperature was fixed at 33°C or 37°C. Clamping the temperature constant after 3 days of temperature cycling markedly reduced the oscillations in MMP activity, an effect evident within the first 36 hours.

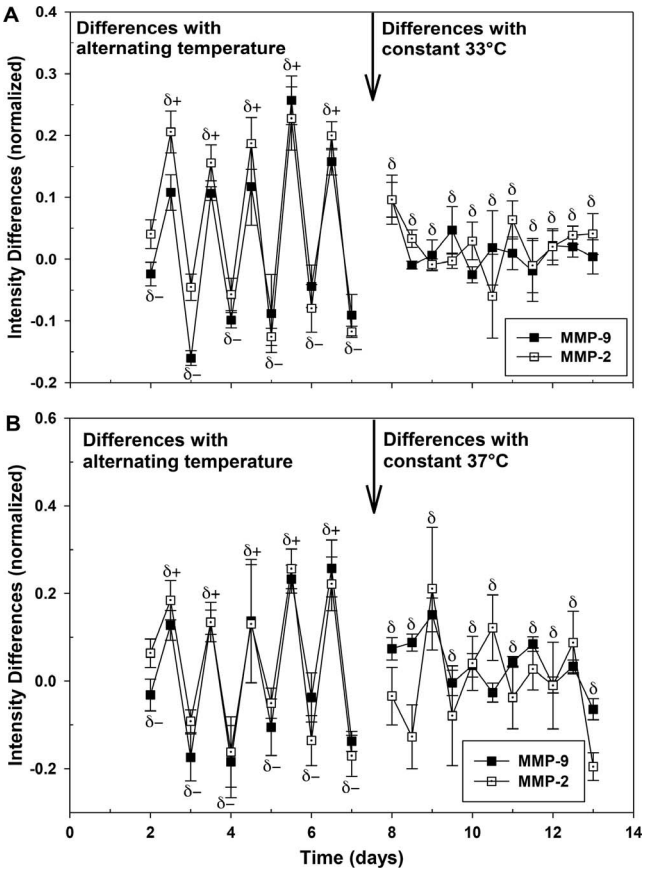

FIGURE 3. Effects of 6 days of temperature cycling on activity of secreted MMP-9 and MMP-2, before and while subsequently clamping temperature at 33°C (**A**) or 37°C (**B**). Data are presented as differences in secretion between successive 12-hour periods. The means ± SEs of (**A**) have been calculated from the replicate measurements from four wells of Figure 2. The means ± SEs of (**B**) have been calculated from replicate measurements conducted in parallel with a separate set of four wells. The differences measured on increasing temperature from 33°C to 37°C are labeled "δ+" and differences observed on reducing temperature from 37°C to 33°C are identified as "δ–." Differences noted between successive measurements at a constant temperature of 33°C or 37°C are labeled "δ." Temperature oscillation significantly drove MMP-9 and MMP-2 secretion oscillation (see text). However, no significant entrainment of those oscillations was detected for either MMP-9 or MMP-2 at constant 33°C or 37°C (see text).

We wondered whether a more sustained period of temperature cycling might be more effective in entraining oscillations in MMP activity before clamping the temperature constant. In the experiment of Figures 2 and 3, temperatures were alternated between 37 and 33°C for 6 days, twice as long as in the experiment of Figure 1. Figure 2B displays MMP intensities measured after each 12-hour interval during that 6-day period. Once again, two-way repeated measures ANOVA detected significant enhancement of the averaged relative intensities of Figure 2B at the higher temperature, for both MMP-9 ($P = 0.001$) and MMP-2 ($P < 0.001$) during the period of temperature cycling. Figure 2A presents a representative zymogram obtained with one of the four wells studied in that experiment. Careful viewing of the zymogram indicates that the intensity and height of each band is greater for collections conducted at 37°C and smaller at 33°C.

The presentation of Figure 3 permits the temperature-driven oscillations in activity of secreted MMP to be visualized more clearly, separated from long-term background drift.

Investigative Ophthalmology & Visual Science

Figure 3 presents the time course of sequential differences in MMP activity over the 6-day temperature cycling. As in Figures 1 and 2, MMP secretion was first normalized to the initial collection sample. Then, the differences in MMP secretion were calculated as the 12-hour secretions collected at any time point (t) minus those collected at the previous time point (t-1) 12 hours earlier. Plotting these differences in secretion as a function of time more clearly revealed the highly significant, temperature-driven oscillations in MMP secretion (Fig. 3). Differences in activity of secreted MMP on increasing temperature from 33°C to 37°C are labeled "δ+" and the secretion differences noted on decreasing the temperature are identified as "δ–." Analyzed by two-way repeated measures ANOVA and the Holm-Sidak test, oscillating differences in activity were significantly associated with temperature cycling during the period of temperature oscillations for both MMP-9 ($P < 0.001$, Fig. 3A, and $P = 0.022$, Fig. 3B) and MMP-2 ($P = 0.001$, Fig. 3A, and $P = 0.031$, Fig. 3B). Averaged for the five experiments conducted, switching between 33 and 37°C produced mean ± SE changes in activity ($n = 436$) of 0.40 ± 0.03 in MMP-9 and 0.22 ± 0.02 in MMP-2.

Clamping the temperature constant markedly dampened the fluctuation magnitude of the differences in zymographic intensity. Fixing the temperature at 33°C reduced the changes in activity of MMP-9 by 60% ± 4% and of MMP-2 by 59% ± 6% (Fig. 3A). Fixing the temperature at 37°C produced comparable effects, reducing changes in activity of MMP-9 by 53% ± 15% and of MMP-2 by 78% ± 6% (Fig. 3B). To address whether the residual fluctuations at constant temperature were influenced by the previous exposure to temperature cycling, data were analyzed with two-way repeated measures ANOVA and then the Holm-Sidak Pairwise Multiple Comparison Procedures. Day was one of the two factors analyzed. The other factor tested was the potentially entrained rhythmicity established by the earlier period of temperature cycling. No significant entrainment was detected for MMP-9 ($P = 0.76$) or MMP-2 ($P = 0.26$) after fixing the temperature at 33°C in the traces of Figure 3A. Likewise, no significant entrainment was observed for MMP-9 ($P = 0.37$) or MMP-2 ($P = 0.74$) after fixing the temperature at 37°C in the traces of Figure 3B. With one exception, no significant dependence on day was noted when the temperatures were clamped at either 33 or 37°C. That exception was the increase in fluctuations noted ($P = 0.004$, Holm-Sidak method) for MMP-9 at days 9 to 10 with the temperature fixed at 37°C (Fig. 3B). The differences in activity of secreted MMP-2 displayed qualitatively similar fluctuations on those days, but day was not a significant factor for MMP-2 at 37°C ($P = 0.28$, Fig. 3B).

Effect of Inhibiting HSF1 on Secretion of MMP-2 and MMP-9

The preceding results (Figs. 1–3) demonstrated that temperature cycling drives oscillations in activity of secreted MMP. The retention of only small subsequent fluctuations in MMP secretion at constant temperature suggested that the temperature effect might be mediated by a direct effect on one or more cell processes, rather than through temperature entrainment of peripheral clock genes. We pursued this possibility with a complementary test of the potential role of clock genes by applying 100 μM KNK437[21,40] to block the action of HSF1, which links temperature oscillations to cycling of peripheral clocks (see Discussion).

Figure 4 displays results averaged from two experiments conducted identically. The KNK437 prevented the upward drift in mean activity of secreted MMP-9 (Fig. 4A) and MMP-2 (Fig. 4B) observed with vehicle-treated control cells, and actually inhibited MMP-9 (Fig. 4A). In each experiment, duplicate measurements of enriched media were conducted and averaged from each of six wells at each time point. The KNK437 reduced the mean activity of secreted MMP-9 by 53% ± 8% in comparison to that of the drug-treated cells in the baseline period ($P < 0.001$, one-way repeated measures ANOVA and Holm-Sidak test after verifying equal variance and normality by the Shapiro-Wilk test). The KNK437 also reduced the temperature-driven oscillations in activity of secreted MMP-9 by 68% ± 9% ($P < 0.001$, using the same statistical approach).

In contrast, KNK437 did not inhibit the mean activity of secreted MMP-2. In comparison with that during the baseline period, the activity of MMP-2 was slightly increased (by 6% ± 4%, $P = 0.003$ using the same statistical analysis). The KNK437 also did not affect the temperature-triggered oscillations. The differences in activity of secreted MMP-2 in the drug-treated cells before and after KNK437 were not normally distributed (Shapiro-Wilk test), but analysis with repeated measures ANOVA on ranks indicated that the probability of the null hypothesis was 0.414.

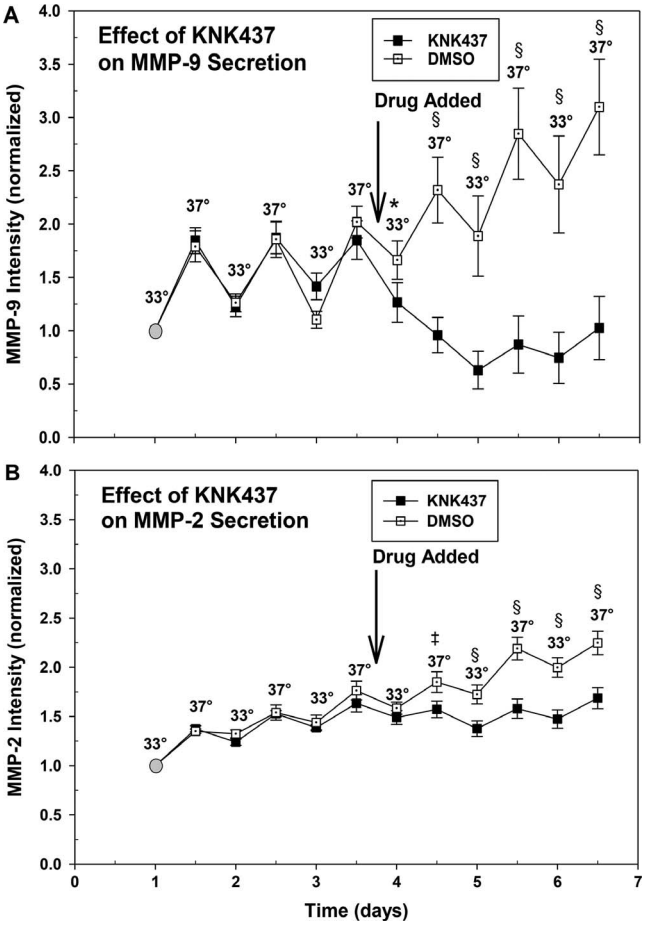

Figure 4. Effect of inhibiting HSF1 with KNK437 on temperature-driven oscillations in activity of secreted MMP. The graphs have been generated by averaging the results of two experiments obtained from replicate measurements of enriched media from six wells each for every time point. Incubation with 100 μM KNK437 inhibited MMP-9 secretion (**A**) and prevented the upward drift of MMP-2 secretion observed with vehicle-treated cells (**B**). The KNK437 also reduced temperature-driven cycling of MMP-9 (**A**) but not of MMP-2 secretion (**B**) (one-way repeated measures ANOVA; see text). The probabilities of the null hypothesis calculated by Student's *t*-test for point comparisons of total activity of secreted MMP are labeled as follows: $^*P < 0.05$, $‡P < 0.01$, and $§P < 0.001$.

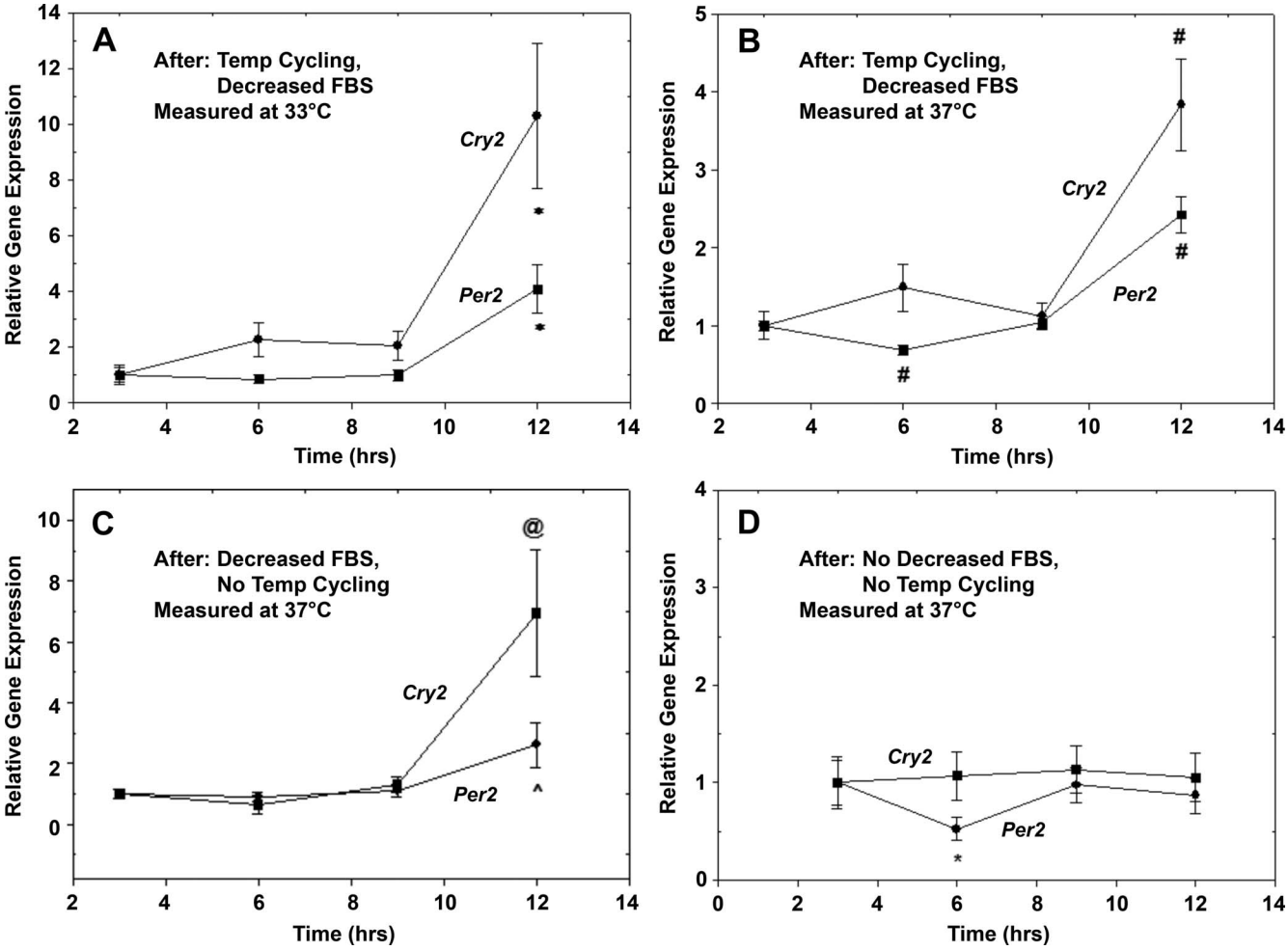

FIGURE 5. Expression of clock genes *Per2* and *Cry2*. *Data points* were generated by averaging three to four replicate qPCR measurements, using the ΔΔCt method. In the experiment of (**A**) and (**B**), cells were initially plated into 10% FBS and 12 hours later incubated in 1% FBS for the rest of the experiment. After initial incubation at 37°C, temperature was switched between 33°C and 37°C every 12 hours for 60 hours, beginning and ending either at 33°C (**A**) or at 37°C (**B**). Cells were analyzed on the final day at the times indicated on the *abscissa*. Irrespective of the phase of temperature cycling, peak expressions of both *Cry2* and *Per2* were observed at 12:00 hours (*$P < 0.02$, #$P < 0.005$, Student's *t*-test). Duplicate qPCR measurements with different cDNA collections from the same cells gave similar results. (**C**) Cells were incubated in 10% FBS for 12 or 24 hours before reducing FBS to 1% (see text). Even in the absence of any temperature cycling, *Cry2* was significantly activated at 12:00 hours of the final day (of RNA collection) (@$P < 0.05$) and there was a trend for an accompanying increase in *Per2* (^$0.1 > P > 0.05$). (**D**) In the absence either of temperature cycling or lowering of the 10% FBS, no activation was noted on the final day of collection. A small, but significant reduction in *Per2* was observed at 6:00 hours (*$P < 0.02$, Student's *t*-test).

Effect of Temperature on Expression of TM-Cell Clock Genes

In addition to the foregoing tests for entrainment and HSF1 inhibition, the potential role of peripheral clock genes in temperature-driven cycling of MMP release was probed by determining whether the clock genes *Per2* and *Cry2* cycle in response to temperature oscillations. These genes are expressed in human TM cells.[41]

In the first experiment (Figs. 5A, 5B), the incubation protocol was qualitatively similar to that of Figure 1. After an initial baseline period of 1 day in 10% FBS at 37°C, temperatures were alternated between 33°C and 37°C at 9 AM and 9 PM over the succeeding 60 hours of incubation in 1% FBS. During the temperature cycling, half the cells were first incubated at 33°C (cells of Fig. 5A) and half were retained at 37°C (cells of Fig. 5B), to initiate oscillations that were 12 hours out of phase. At 3-hour intervals during the last 12 hours of incubation (Figs. 5A, 5B), RNA was collected from both sets of cells. Three to four replicates were analyzed for each time point. The qPCR measurements were normalized to the first data point of each temperature cycle. Both *Cry2* and *Per2* displayed enhanced gene expression at 12 hours (9 PM of the final day), regardless of whether the cells had been incubating at 33°C or 37°C. The probabilities of the null hypothesis, that the relative gene expression was one, were less than 0.02 at 33°C (Fig. 5A) and less than 0.005 at 37°C (Fig. 5B) for both *Cry2* and *Per2* by Student's *t*-test. The peaks in gene expression did not correspond to the temperature cycle because the measurements of Figure 5A were conducted at 33°C, whereas the measurements of Figure 5B were obtained at 37°C. Duplicate qPCR measurements obtained with different cDNA collections from the same cells led to similar results. These data suggested that the observed synchrony of *Cry2* and *Per2* clock-gene expression was not the result of the associated temperature cycling. *Per2* also displayed a small but significant fall in gene expression after 6 hours of incubation at 37°C (Fig. 5B, $P < 0.005$, Student's *t*-test), but that change was unaccompanied by a corresponding change in *Cry2* expression.

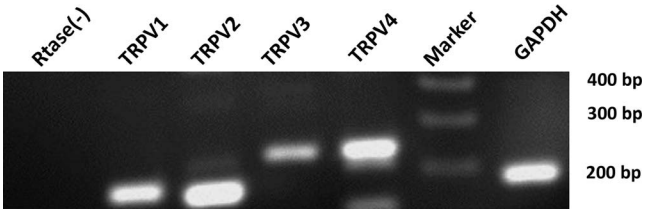

FIGURE 6. Expression of TRPV1-4 channels detected by RT-PCR. Omission of reverse-transcriptase (RTase[−]) eliminated product, verifying that the cDNA contained no significant DNA contamination. The internal control was GAPDH. Similar results were obtained in a duplicate experiment conducted with RNA obtained from different cells.

To verify that the changes in clock-gene expression (Figs. 5A, 5B) were not driven by the temperature cycling, qPCR measurements were conducted in a second experiment without temperature oscillations. All cells were first plated into medium containing 10% FBS at 37°C. The FBS was then reduced to 1% after either 12 or 24 hours of exposure to the 10% concentration. The total incubation time was identical (60 hours) for the two sets of cells before the day of RNA collection. The *Cry2* of cells incubated in 1% FBS for 48 hours again displayed a peak gene expression at 12 hours in three replicates (Fig. 5C, $P < 0.05$, Student's *t*-test). The *Per2* also displayed a trend toward a peak gene expression at 12 hours in three replicates (Fig. 5C, $0.1 > P > 0.05$, Student's *t*-test). These results supported the conclusion that temperature cycling was not necessary to elicit the observed time course in gene expression noted in Figures 5A and 5B. Rather, the peaks observed could have reflected either responses to lowering FBS concentration[42] or spontaneous clock-gene cycling.

In a third experiment, the potential role of changes in FBS concentration was tested. Clock-gene expression was measured by qPCR after incubating cells in 10% FBS for 60 hours at a fixed temperature of 37°C. In contrast to Figures 5A through C, measuring gene expression at the same times on the day of collection revealed no cycling of *Per2* or *Cry2* (Fig. 5D). The results suggested that the activated clock-gene expression displayed in Figures 5A through C was triggered by changes in FBS concentration, and did not reflect spontaneous synchronized cycling in the cultured hTM5 cells. This conclusion was further supported by the results of a fourth experiment in which temperature was again held constant at 37°C and the FBS concentration was 10%. Following an initial preincubation period of 24 hours, the qPCR measurements were conducted at the same times as in Figure 5D, but during 3 consecutive days. Once again, no consistent changes were noted in the time courses of *Per2* and *Cry2* expression (results not shown). These data suggested that lowering FBS concentration initiates synchronous oscillations of clock-gene expression.

Effect of Inhibiting Temperature-Sensitive Ion Channels

The preceding results suggested that temperature cycling did not produce synchronized cycling of clock genes in the cultured TM cells (see Discussion). An alternative possibility was that the oscillations in secretion could possibly reflect direct actions of temperature on temperature-sensitive channels, thereby triggering signaling cascades. Ion channels that have been thought to display mode changes over physiologically relevant temperatures are TRPV1, TRPV3, TRPV4, and TRPM8,[23] although doubts have been raised about whether TRPV3 and TRPV4 are functional thermosensors.[43] The TRPV2

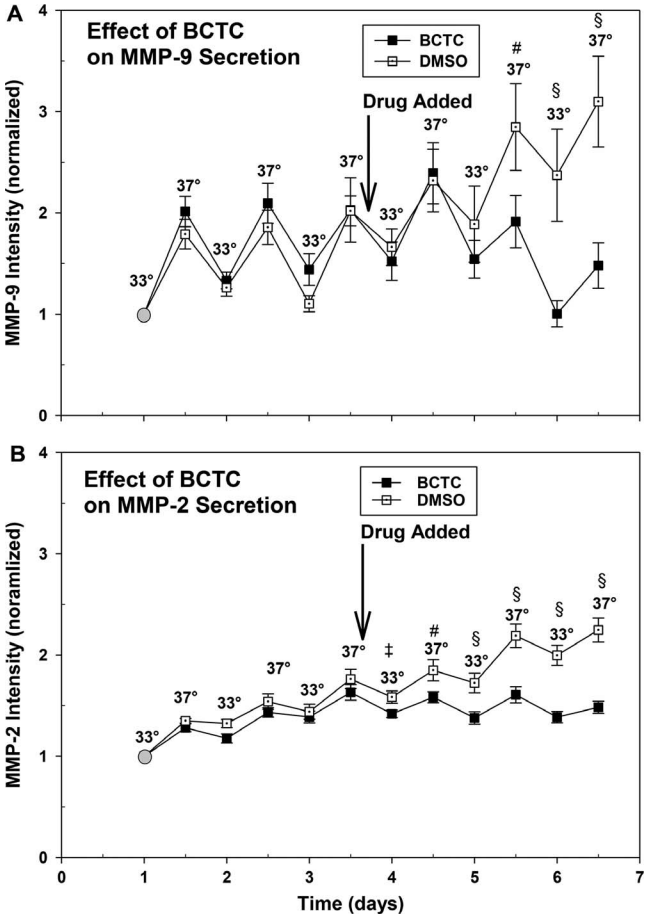

FIGURE 7. Effect of BCTC on activity of secreted MMP. As in Figure 1, secretion was measured during 12-hour periods at alternating temperatures of 33° and 37°C. Drug or vehicle (DMSO) was added at the *vertical arrows*. Data from both the drug- and vehicle-treated cells were obtained by averaging the results of two experiments, each conducted with replicate measurements from six wells. At 10 μM, BCTC partially inhibited mean activity of secreted MMP-9 (**A**) and prevented the upward drift in mean activity of secreted MMP-2 (**B**) in comparison with the vehicle-treated cells. The BCTC did not significantly alter the magnitude of the temperature-driven oscillations noted in the control period for either MMP-9 or MMP-2 (see text).

to 4 and at least one splice variant of TRPV1 are expressed in the TM.[41] The probability of gene expression of the cold-sensitive TRPM8 channel is less secure.[41] We verified the expression of TRPV1 to 4 in hTM5 cells by RT-PCR (Fig. 6).

We addressed the possibility that these channels might play a mediating role in the temperature-driven oscillations in activity of secreted MMP by applying channel inhibitors. We initially applied ruthenium red, which inhibits TRPV1 to 4, among other channels. However, prolonged exposure to this drug over periods of days markedly reduced cell viability. In contrast, the TM cells tolerated prolonged exposure to 10 μM BCTC. At this concentration, BCTC primarily abolished the upward drift of both MMP-9 (Fig. 7A) and MMP-2 (Fig. 7B) noted with the vehicle-treated controls. In addition, comparison of the data from the drug-treated cells before and after adding BCTC indicated that the inhibitor partially reduced the mean activity of secreted MMP-9 ($P = 0.024$, one-way repeated measures ANOVA followed by Holm-Sidak test). At the conclusion of the experiment (at 6.5 days), secreted activity of both MMP-9 and MMP-2 were approximately 50% lower in the BCTC-treated cells than in the cells exposed to vehicle

alone. However, analysis by paired *t*-test indicated that BCTC did not significantly change the temperature-driven oscillations in activity of MMP-2 ($P = 0.591$) observed during the control period. The paired MMP-9 data did not pass the Shapiro-Wilk normality test, so that those results were analyzed with the Wilcoxon signed rank test. The latter test suggested that the temperature-driven oscillations in MMP-9 also were unaffected by the BCTC ($P = 0.063$).

At 10 μM, BCTC inhibits both TRPM8 and TRPV1.[33] To distinguish between these two targets in having mediated the secreted MMP activity, we examined the effect of HC 067047, which at 1- and 10-μM concentration inhibits both TRPM8 and TRPV4 channels.[34] At these concentrations, HC 067047 did not alter cell viability and affected activity of neither secreted MMP-9 nor MMP-2 (data not shown). Because TRPM8 was a target common to both BCTC and HC 067047, but only BCTC was effective, the results suggested that the other BCTC target, TRPV1 channels, may play a role in mediating total activity of secreted MMP-2, albeit not its temperature-driven oscillations.

Discussion

The central finding of the current work is that small, likely physiologically relevant oscillations in temperature do drive oscillations in activity of secreted MMP-9 and MMP-2 by cultured hTM5 cells. Two considerations led us to cycle the temperature between 37 and 33°C. First, the central clock cycles core temperature of healthy human subjects by 2 to 4°C.[20,21,44] Second, the temperature of the TM cells also must be strongly affected by the nearby corneal surface temperature when the eyelids are open. Under this condition, the mean ocular surface temperature of healthy subjects has been estimated from infrared ocular thermograms to be 31.9 ± 0.5°C (mean ± SE) at room temperature.[45] Geiser et al.[46] reported a similar value (32.7 ± 0.3°C) in young healthy subjects using the same technique. That value depended strongly on ambient temperature, falling to 26.4 ± 0.9°C at −20°C and rising to 36.2 ± 0.5°C at 40°C. The infrared results underestimate corneal cell temperature, as the measurements reflect the temperature of the tear film surface. Increasing depth of that film will shift temperature at the cell surface closer to the core body temperature. Estimates based on a theoretical model suggest that even the retinal temperature varies significantly from 35.2°C to 37.1°C at ambient temperatures of −20°C and 40°C, respectively.[46] The TM-cell temperature must lie between the corresponding values at the corneal surface and at the retina. Subject to these uncertainties, the temperature cycling chosen, alternating between 37°C and 33°C, is likely to be physiologically relevant.

The observation that a small temperature drop inhibits activity of secreted MMP was by no means predictable, given available data from more extreme temperature changes than those studied here. Temperature might affect protein formation, flux through the Golgi complex, and accessibility to the plasma membrane, as well as secretion. For instance, reducing temperature from 37 to 26°C markedly accelerates Golgi processing of mutant CFTR ΔF508 protein expressed in NIH 3T3 cells within 12 hours.[47] A much larger temperature reduction to 4°C has specifically stimulated MMP secretion from hepatic sinusoidal endothelial cells within 30 minutes by inducing actin disassembly.[48] The temperature dependence of the actin cytoskeleton is expected to be highly dependent on cell type, activity, and topography. For example, cooling to 4°C rapidly disassembles F-actin within lamellipodia of chemoattractant-stimulated polymorphonuclear leukocytes, but has little effect on unstimulated cells, in which the turnover of F-actin is much lower.[49] Confocal microscopy and immunohistochemistry specifically of TM cells, both human and porcine, have demonstrated that MMP-2 colocalizes with podosome- or invadopodia-like structures (PILS) that may serve as foci for extracellular matrix turnover.[50] The effect of temperature on MMP-2 secretion at PILS or elsewhere on TM-cell plasma membranes is unknown.

In principle, temperature cycling initiated by the central clock and eyelid position during the diurnal and nocturnal hours could drive cycling of MMP secretion either by acting directly on temperature-sensitive targets, such as temperature-sensitive ion channels, or by synchronizing the peripheral clock genes of the TM cells. Three current results argue against mediation by the peripheral clock of the TM. First, 3 to 6 days of temperature cycling did not significantly entrain oscillation in MMP secretion after the incubation temperature was clamped constant. Second, interrupting the link between temperature oscillations and clock-gene activation by blocking HSF1 reduced temperature-driven cycling of MMP-9, but not of MMP-2, activity. The HSF1 oligomerizes in response to temperature jumps[21] and functions as a circadian transcription factor.[25] The inhibitor KNK437 prevents temperature-triggered increases in HSF1 mRNA[40] and inhibits the responses of peripheral clocks to changes in temperature.[20,21] Third, we were unable to document temperature-driven cycling of the TM clock genes *Per2* and *Cry2*. The activations observed of these clock genes could be ascribed to the accompanying reductions in FBS from 10% to 1%, performed to minimize changes in gene expression associated with cell division. Shifts in serum concentration have been reported to trigger circadian changes in cultured cells.[42] No activation of *Per2* and *Cry2* was noted when cells were incubated at constant 10% FBS and at constant temperature. Thus, these clock genes do not appear to cycle synchronously in cultured hTM5 cells and are apparently not activated or cycled by alternating temperature between 33 and 37°C. We cannot exclude the possibility that oscillations occur spontaneously in single hTM5 cells, but are not synchronized across cells. This would account for the lack of detectable oscillations in the population.

Expression levels specifically of *Per* and *Cry* were assayed in this study. These are the most robust "cyclers" in the core feedback loop of the clock, and therefore provide a reliable readout of the molecular clock. Expression of *BMal1* mRNA is rhythmic, but the cycling is not as robust as that of *Per* and *Cry*, and in addition, clock function can persist in the absence of this cycling.[51] We acknowledge that other clock genes (e.g., *rev erb α*) could be involved in the response to temperature, but their involvement would likely reflect a noncircadian function, as core components of the clock (*Per*, *Cry*) are not affected.

Insofar as the temperature-driven oscillations in activity of secreted MMP-9 and MMP-2 do not appear to be mediated by clock-gene cycling in TM cells, we addressed the possibility that the oscillations might result from signaling cascades initiated by temperature-sensitive ion channels. Of particular interest is the TRP family of channels, which includes 28 mammalian members.[43] The TRP channels are nonselective cation channels, which can function in the plasma and intracellular membranes and can be activated by both physical and chemical stimuli.[43] Although a number of other ion channels display some temperature sensitivity,[52] temperature-responsive TRP channels are of particular interest because they exhibit unusually large thermal sensitivity and constitute the primary temperature sensors in mammalian sensory nerve endings.[23,53,54] Three subfamilies, the vanilloid TRPV channels and the melastatin TRPM and the canonical TRPC channels include at least one temperature-sensitive member (thermoTRP).[43] Of these thermoTRPs, the heat-sensitive TRPV1 and the cold-sensitive TRPM8 channels are most likely relevant

Investigative Ophthalmology & Visual Science

to the physiologic temperature shifts of TM cells. Activation temperatures for TRPV1 and TRPM8 have been cited to be higher than 43°C and lower than 28°C, respectively.[23] Those activation temperatures may be modified by ambient conditions to be more closely physiologically relevant. For example, very strong depolarization activates TRPV1 even at room temperature.[23] Extracellular protons also have been suggested to facilitate gating movement by disrupting hydrogen bonds, sensitizing TRPV1 channels to smaller temperature changes.[55] These shifts in activation temperature likely reflect induced changes in the specific heat capacity during ion gating.[52,56] The gene TRPV1 is expressed, but the probability of TRPM8 expression is much lower in TM cells.[41] We have verified gene expression of TRPV1-4 in hTM5 cells by RT-PCR (Fig. 6).

The blocker HC 067047 is a potent, selective inhibitor of hTRPV4. This compound inhibits human TRPV4 with the half maximal inhibitory concentration (IC_{50}) = 48 ± 6 nM (mean ± SE). The HC 067047 does not inhibit other TRPV isoforms at concentrations up to 5 μM. The HC 067047 inhibits the human ether-à-go-go–related gene channel and the menthol receptor TRPM8 with IC_{50} values of 370 and 780 nM, respectively.[34] In contrast, the compound BCTC has been regarded as a potent, selective inhibitor of hTRPV1, with an IC_{50} of 2.6 ± 1.2 μM,[33,57] but also inhibits mouse TRPM8 (IC_{50} of 0.8 ± 1.0 μM).[33] In the present work, BCTC, but not HC 067047, inhibited total MMP activity, suggesting that TRPV1 may play a role in modulating that secretion. However, inhibition of TRPV1 did not modify the temperature-dependent oscillations in secreted MMP-2 and MMP-9 activity.

In summary, we have measured activity of secreted MMP-2 and MMP-9 by isolated hTM5 cells as an index of TM-cell function in modulating outflow facility in vivo. Cycling temperature over a small, likely physiologically relevant range produced activity changes of approximately 40% in secreted MMP-9 and approximately 20% in secreted MMP-2. The mechanism linking cycling of temperature to MMP secretion is unclear. Our data indicate that neither synchronous cycling of TM clock genes *Per2* and *Cry2* nor temperature-sensitive TRP channels mediate temperature-driven cycling of secreted MMP-9 and MMP-2 activity. Still, temperature-sensitive TRP channels may prove important in the potential temperature-dependent secreted activity of other MMPs and of TIMPs (tissue inhibitors of MMPs).

Our current results point to a promising new area for investigation to dissect the circadian biology of aqueous humor dynamics. Our approach warrants extension to primary cultures of human TM cells and to TM in situ, and consideration of additional MMPs and TIMPs.

Acknowledgments

The authors thank Terry A. Braun, PhD, University of Iowa, Iowa City, Iowa, United States; Abbot Clark, PhD, University of North Texas HSC, Fort Worth, Texas, United States; and Gui-shaung Ying, PhD, University of Pennsylvania, Philadelphia, Pennsylvania, United States for helpful discussions.

Supported by National Institutes of Health Research Grant EY13624 (MMC), the Mackall Foundation Trust and Research to Prevent Blindness (RAS), Core Grant EY13624 (MMC and RAS), and Grant G-YK88 from The Hong Kong Polytechnic University (SKL).

Disclosure: **S.K. Li**, None; **J. Banerjee**, None; **C. Jang**, None; **A. Sehgal**, None; **R.A. Stone**, None; **M.M. Civan**, None

References

1. Brubaker RF. Clinical measurement of aqueous dynamics: implications for addressing glaucoma. In: Civan MM, ed. *Eye's Aqueous Humor: From Secretion to Glaucoma*. San Diego: Academic Press; 1998:234–284.
2. Asejczyk-Widlicka M, Pierscionek BK. Fluctuations in intraocular pressure and the potential effect on aberrations of the eye. *Br J Ophthalmol*. 2007;91:1054–1058.
3. Liu JH. Circadian rhythm of intraocular pressure. *J Glaucoma*. 1998;7:141–147.
4. Liu H, Fan S, Gulati V, et al. Aqueous humor dynamics during the day and night in healthy mature volunteers. *Arch Ophthalmol*. 2011;129:269–275.
5. Sit AJ, Nau CB, McLaren JW, Johnson DH, Hodge D. Circadian variation of aqueous dynamics in young healthy adults. *Invest Ophthalmol Vis Sci*. 2008;49:1473–1479.
6. Nau CB, Malihi M, McLaren JW, Hodge DO, Sit AJ. Circadian variation of aqueous humor dynamics in older healthy adults. *Invest Ophthalmol Vis Sci*. 2013;54:7623–7629.
7. Blondeau P, Tetrault JP, Papamarkakis C. Diurnal variation of episcleral venous pressure in healthy patients: a pilot study. *J Glaucoma*. 2001;10:18–24.
8. Becker B, Constant MA. The facility of aqueous outflow; a comparison of tonography and perfusion measurements in vivo and in vitro. *AMA Arch Ophthalmol*. 1956;55:305–312.
9. Brubaker RF. The effect of intraocular pressure on conventional outflow resistance in the enucleated human eye. *Invest Ophthalmol*. 1975;14:286–292.
10. Camras LJ, Stamer WD, Epstein D, Gonzalez P, Yuan F. Differential effects of trabecular meshwork stiffness on outflow facility in normal human and porcine eyes. *Invest Ophthalmol Vis Sci*. 2012;53:5242–5250.
11. Dijkstra BG, Ruijter JM, Hoyng PF. Outflow characteristics of isolated anterior segments of human eyes. *Invest Ophthalmol Vis Sci*. 1996;37:2015–2021.
12. Ellingsen BA, Grant WM. The relationship of pressure and aqueous outflow in enucleated human eyes. *Invest Ophthalmol*. 1971;10:430–437.
13. Francois J, Rabaey M, Neetens A, Evens L. Further perfusion studies on the outflow of aqueous humor in human eyes. *AMA Arch Ophthalmol*. 1958;59:683–691.
14. Hashimoto JM, Epstein DL. Influence of intraocular pressure on aqueous outflow facility in enucleated eyes of different mammals. *Invest Ophthalmol Vis Sci*. 1980;19:1483–1489.
15. Nihard P. Influence of ocular pressure on resistance to flow of aqueous humor [in French]. *Acta Ophthalmol (Copenh)*. 1962;40:12–27.
16. Yoshitomi T, Gregory DS. Ocular adrenergic nerves contribute to control of the circadian rhythm of aqueous flow in rabbits. *Invest Ophthalmol Vis Sci*. 1991;32:523–528.
17. Panda S, Antoch MP, Miller BH, et al. Coordinated transcription of key pathways in the mouse by the circadian clock. *Cell*. 2002;109:307–320.
18. Miller BH, McDearmon EL, Panda S, et al. Circadian and CLOCK-controlled regulation of the mouse transcriptome and cell proliferation. *Proc Natl Acad Sci U S A*. 2007;104:3342–3347.
19. Hughes ME, DiTacchio L, Hayes KR, et al. Harmonics of circadian gene transcription in mammals. *PLoS Genet*. 2009;5:e1000442.
20. Buhr ED, Yoo SH, Takahashi JS. Temperature as a universal resetting cue for mammalian circadian oscillators. *Science*. 2010;330:379–385.
21. Edery I. Circadian rhythms. Temperatures to communicate by. *Science*. 2010;330:329–330.
22. Mapstone R. Thermometry and the eye. *Trans Ophthalmol Soc U K*. 1969;88:693–699.
23. Voets T, Droogmans G, Wissenbach U, Janssens A, Flockerzi V, Nilius B. The principle of temperature-dependent gating in

cold- and heat-sensitive TRP channels. *Nature*. 2004;430:748–754.

24. Schmutz I, Ripperger JA, Baeriswyl-Aebischer S, Albrecht U. The mammalian clock component PERIOD2 coordinates circadian output by interaction with nuclear receptors. *Genes Dev*. 2010;24:345–357.
25. Reinke H, Saini C, Fleury-Olela F, Dibner C, Benjamin IJ, Schibler U. Differential display of DNA-binding proteins reveals heat-shock factor 1 as a circadian transcription factor. *Genes Dev*. 2008;22:331–345.
26. Quigley HA. Number of people with glaucoma worldwide. *Br J Ophthalmol*. 1996;80:389–393.
27. Bradley JM, Vranka J, Colvis CM, et al. Effect of matrix metalloproteinases activity on outflow in perfused human organ culture. *Invest Ophthalmol Vis Sci*. 1998;39:2649–2658.
28. Crosson CE, Sloan CF, Yates PW. Modulation of conventional outflow facility by the adenosine A1 agonist N6-cyclohexyladenosine. *Invest Ophthalmol Vis Sci*. 2005;46:3795–3799.
29. Li A, Banerjee J, Peterson-Yantorno K, Stamer WD, Leung CT, Civan MM. Effects of cardiotonic steroids on trabecular meshwork cells: search for mediator of ouabain-enhanced outflow facility. *Exp Eye Res*. 2012;96:4–12.
30. Pang IH, Shade DL, Clark AF, Steely HT, DeSantis L. Preliminary characterization of a transformed cell strain derived from human trabecular meshwork. *Curr Eye Res*. 1994;13:51–63.
31. Valenzano KJ, Grant ER, Wu G, et al. N-(4-tertiarybutylphenyl)-4-(3-chloropyridin-2-yl)tetrahydropyrazine-1(2H)-carbox-amide (BCTC), a novel, orally effective vanilloid receptor 1 antagonist with analgesic properties: I. In vitro characterization and pharmacokinetic properties. *J Pharmacol Exp Ther*. 2003;306:377–386.
32. Pomonis JD, Harrison JE, Mark L, Bristol DR, Valenzano KJ, Walker K. N-(4-Tertiarybutylphenyl)-4-(3-cholorphyridin-2-yl)-tetrahydropyrazine-1(2H)-carbox-amide (BCTC), a novel, orally effective vanilloid receptor 1 antagonist with analgesic properties: II. In vivo characterization in rat models of inflammatory and neuropathic pain. *J Pharmacol Exp Ther*. 2003;306:387–393.
33. Behrendt HJ, Germann T, Gillen C, Hatt H, Jostock R. Characterization of the mouse cold-menthol receptor TRPM8 and vanilloid receptor type-1 VR1 using a fluorometric imaging plate reader (FLIPR) assay. *Br J Pharmacol*. 2004;141:737–745.
34. Everaerts W, Zhen X, Ghosh D, et al. Inhibition of the cation channel TRPV4 improves bladder function in mice and rats with cyclophosphamide-induced cystitis. *Proc Natl Acad Sci U S A*. 2010;107:19084–19089.
35. Sanka K, Maddala R, Epstein DL, Rao PV. Influence of actin cytoskeletal integrity on matrix metalloproteinase-2 activation in cultured human trabecular meshwork cells. *Invest Ophthalmol Vis Sci*. 2007;48:2105–2114.
36. Hawkes SP, Li H, Taniguchi GT. Zymography and reverse zymography for detecting MMPs and TIMPs. *Methods Mol Biol*. 2010;622:257–269.
37. Hu X, Beeton C. Detection of functional matrix metalloproteinases by zymography. *J Vis Exp*. 2010;45:2445.
38. Li A, Leung CT, Peterson-Yantorno K, Stamer WD, Civan MM. Cytoskeletal dependence of adenosine triphosphate release by human trabecular meshwork cells. *Invest Ophthalmol Vis Sci*. 2011;52:7996–8005.
39. Lee CS, Shin YJ, Won C, et al. Simvastatin acts as an inhibitor of interferon gamma-induced cycloxygenase-2 expression in human THP-1 cells, but not in murine RAW264.7 cells. *Biocell*. 2009;33:107–114.
40. Yokota S, Kitahara M, Nagata K. Benzylidene lactam compound, KNK437, a novel inhibitor of acquisition of thermotolerance and heat shock protein induction in human colon carcinoma cells. *Cancer Res*. 2000;60:2942–2948.
41. Wagner AH, Anand VN, Wang WH, et al. Exon-level expression profiling of ocular tissues. *Exp Eye Res*. 2013;111:105–111.
42. Balsalobre A, Damiola F, Schibler U. A serum shock induces circadian gene expression in mammalian tissue culture cells. *Cell*. 1998;93:929–937.
43. Nilius B, Szallasi A. Transient receptor potential channels as drug targets: from the science of basic research to the art of medicine. *Pharmacol Rev*. 2014;66:676–814.
44. Sandstrom ME, Madden LA, Taylor L, et al. Variation in basal heat shock protein 70 is correlated to core temperature in human subjects. *Amino Acids*. 2009;37:279–284.
45. Morgan PB, Tullo AB, Efron N. Infrared thermography of the tear film in dry eye. *Eye*. 1995;9:615–618.
46. Geiser MH, Bonvin M, Quibel O. Corneal and retinal temperatures under various ambient conditions: a model and experimental approach. *Klin Monbl Augenheilkd*. 2004;221:311–314.
47. Denning GM, Anderson MP, Amara JF, Marshall J, Smith AE, Welsh MJ. Processing of mutant cystic fibrosis transmembrane conductance regulator is temperature-sensitive. *Nature*. 1992;358:761–764.
48. Upadhya GA, Strasberg SM. Evidence that actin disassembly is a requirement for matrix metalloproteinase secretion by sinusoidal endothelial cells during cold preservation in the rat. *Hepatology*. 1999;30:169–176.
49. Cassimeris L, McNeill H, Zigmond SH. Chemoattractant-stimulated polymorphonuclear leukocytes contain two populations of actin filaments that differ in their spatial distributions and relative stabilities. *J Cell Biol*. 1990;110:1067–1075.
50. Aga M, Bradley JM, Keller KE, Kelley MJ, Acott TS. Specialized podosome- or invadopodia-like structures (PILS) for focal trabecular meshwork extracellular matrix turnover. *Invest Ophthalmol Vis Sci*. 2008;49:5353–5365.
51. Preitner N, Damiola F, Lopez-Molina L, et al. The orphan nuclear receptor REV-ERBalpha controls circadian transcription within the positive limb of the mammalian circadian oscillator. *Cell*. 2002;110:251–260.
52. Chowdhury S, Jarecki BW, Chanda B. A molecular framework for temperature-dependent gating of ion channels. *Cell*. 2014;158:1148–1158.
53. Clapham DE. TRP channels as cellular sensors. *Nature*. 2003;426:517–524.
54. Voets T, Nilius B. TRPs make sense. *J Membr Biol*. 2003;192:1–8.
55. Cao E, Liao M, Cheng Y, Julius D. TRPV1 structures in distinct conformations reveal activation mechanisms. *Nature*. 2013;504:113–118.
56. Clapham DE, Miller C. A thermodynamic framework for understanding temperature sensing by transient receptor potential (TRP) channels. *Proc Natl Acad Sci U S A*. 2011;108:19492–19497.
57. Smart D, Jerman JC, Gunthorpe MJ, et al. Characterisation using FLIPR of human vanilloid VR1 receptor pharmacology. *Eur J Pharmacol*. 2001;417:51–58.

Investigative Ophthalmology & Visual Science